J. Fluid Mech. (1981), *vol.* 112, *pp.* 283–296
Printed in Great Britain

The three-dimensional boundary layer on a rotating helical blade

By PHILIP J. MORRIS

Associate Professor of Aerospace Engineering, 233-L Hammond Building,
The Pennsylvania State University, University Park, PA 16802

(Received 15 December 1980)

The development of a laminar boundary layer on a twisted helical blade is described. An appropriate co-ordinate system is developed in which the boundary-layer equations have a relatively simple form. The choice of blade geometry and the free-stream conditions result in a constant-pressure flow. This permits the flow to be considered the analogue, in a rotating frame, of the zero-pressure-gradient flat-plate boundary layer in a stationary frame. The boundary-layer equations are solved using a double series expansion in powers of distance from the leading edge and the cosine of the blade twist angle. Chordwise and spanwise velocity profiles are calculated. The variation in the skin friction coefficients is calculated as a function of position on the blade.

1. Introduction

The simplest application of the boundary-layer equations is for the flow along a thin flat plate in a uniform parallel stream. Owing to the simplicity of this solution it has provided a basic flow to which various parametric perturbations may be applied. One example is the understanding of the initial stages of transition from laminar to turbulent flow in boundary layers obtained by applying linear perturbations to the flat-plate boundary-layer flow and observing, or calculating, their subsequent growth or decay. Further developments considering such effects as pressure gradients, curvature, or compressibility have not altered the understanding gained by examining the simplest primary flow.

Such simplicity is rarely offered in the study of three-dimensional boundary layers. However the flow about a disk rotating in a fluid at rest or the boundary layer on a yawed cylinder where the potential flow is a function of only one co-ordinate are problems whose solutions may be obtained by solving systems of ordinary differential equations. A number of solutions have been obtained for boundary layers on rotating surfaces. Fogarty (1951) studied the boundary layer on a semi-infinite flat plate rotating about an axis perpendicular to its plane and passing through its edge. The solution obtained was valid far from the axis of rotation but was extended by Tan (1953) to regions nearer this axis. The problem of boundary layers on rotating blades such as those on rotors in axial flow compressors was considered by Horlock & Wordsworth (1965). Since such rotor blades are twisted about the leading edge such that the angle of attack with the oncoming stream varies with radial position, Horlock & Wordsworth introduced a co-ordinate system more suited to the geometry of their

helical blade. In this co-ordinate system a point in the blade surface was specified by x, the distance from the leading edge along a helical generator of the blade, and z, the radius of this helix. Points away from the surface were specified by y, their distance from the surface along a helix orthogonal to the blade surface. The (x, y, z) co-ordinates formed a non-orthogonal system. Though Horlock & Wordsworth obtained the boundary-layer equations in this system, solutions were only obtained for a fixed blade twist angle. Though this accounted for blade stagger it ignored the effects of blade twist. Both Lakshminarayana, Jabbari & Yamaoka (1972) and Yamamoto & Toyokura (1974) used the same non-orthogonal co-ordinate system in their momentum integral studies of turbulent boundary layers on helical blades. Miyake & Fujita (1974) considered a rotating blade which was twisted, with the centre of twist at the blade leading edge, so that the angle of attack was zero along the leading edge. The co-ordinate system used to analyse this problem was also non-orthogonal. The generators of the blade in their model were straight lines subtended at the blade leading edge, so that the blade had no streamwise curvature. For the simplest assumed free-stream flow in which streamlines were helices whose angle equalled the blade twist angle at a given radius the blade was slightly loaded. Miyake & Fujita noted that in order to analyse the effect purely of three-dimensionality of a blade the best way would be to adopt a helical blade with constant velocity along a blade element with the pressure constant everywhere in the flow field. Such an analysis is provided by the present paper.

In the present paper the laminar boundary layer on a twisted helical blade is considered. Though the blade geometry is the same as that proposed by Horlock & Wordsworth (1965) the blade is twisted about the leading edge in the manner of Miyake & Fujita (1974). This geometry is such that there is no spanwise or streamwise pressure gradient for the free-stream flow described above. Thus the flow may be considered to be the analogue, in a rotating reference frame, of the flat-plate boundary layer in a stationary frame. It is shown that a co-ordinate system which is orthogonal in the blade surface may be developed and with the appropriate scaling of the dependent variables a solution for the boundary-layer flow is readily obtained.

2. Analysis

Consider the boundary layer developing on the surface of the helical blade shown in the inset of figure 1. The corresponding co-ordinate systems are shown in figure 1. A point on the surface may be described by

$$\mathbf{r} = z\sin\theta\mathbf{i} + x\cos\phi\mathbf{j} + z\cos\theta\mathbf{k}, \tag{1}$$

where z is the radial distance measured from the ξ_2 axis, θ is the polar angle measured about the ξ_2 axis in a clockwise sense with $\theta = 0$ coinciding with the ξ_3 axis, and x is the distance measured along a helix of radius z and helix angle ϕ. If the external flow at the leading edge is U in the ξ_2 direction and the blade, whose leading edge is along the ξ_3 axis, rotates with an angular velocity Ω in a counter-clockwise sense about the ξ_2 axis, then for zero angle of incidence at the leading edge

$$\tan\phi = \Omega z/U. \tag{2}$$

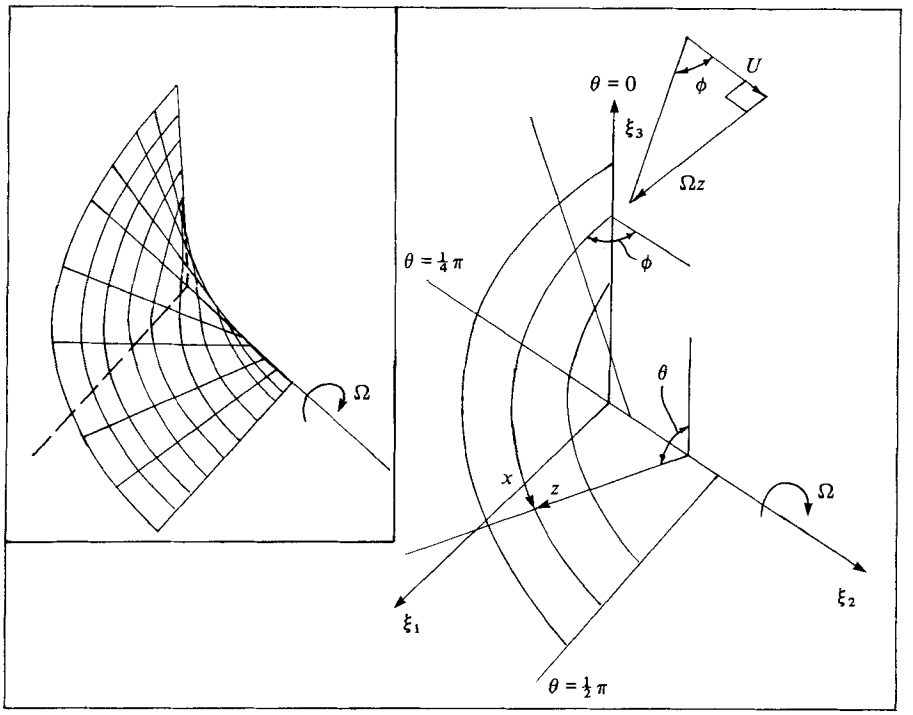

FIGURE 1. Blade surface co-ordinate system with inset showing sketch of the twisted helical blade.

Using the relationship between θ and ϕ, $\theta = x \sin\phi/z$, a general point on the surface is given by

$$\mathbf{r} = z\sin\theta\mathbf{i} + z\theta\cot\phi\mathbf{j} + z\cos\theta\mathbf{k}. \tag{3}$$

However,

$$z\cot\phi = U/\Omega = a, \tag{4}$$

where a is a constant. So that, finally,

$$\mathbf{r} = z\sin\theta\mathbf{i} + a\theta\mathbf{j} + z\cos\theta\mathbf{k}. \tag{5}$$

The surface described by these points is called a 'screw surface'. It is clear that, in spite of the apparent complicated curvature of the surface, lines of constant θ in the blade surface are straight lines. The co-ordinate n is taken as normal to the surface. It is then readily shown that a general point away from the blade is described by

$$\mathbf{r} = (z\sin\theta - n\cos\theta\cos\phi)\,\mathbf{i} + (a\theta + n\sin\phi)\,\mathbf{j} + (z\cos\theta + n\sin\theta\cos\phi)\,\mathbf{k}. \tag{6}$$

The (z, θ, n) co-ordinate system is found to be orthogonal in the blade surface, $n = 0$, and for $\cos\phi = 0$, which corresponds to large radius. By this description alone the present co-ordinate system may not appear to hold any advantages over that used by Miyake & Fujita (1974); however, as will be seen below, the present system allows us to describe a helical blade in co-ordinates which coincide with the directions of interest, both streamwise and chordwise. The boundary-layer equations for this geometry may then be readily obtained from either the boundary-layer equations in generalized co-ordinates (see Michal 1947) or from their vector form with the stretching factors

obtained from (5). It should be noted that in developing the boundary-layer equations only a definition of a surface point is required.

The three-dimensional boundary-layer equations are found to be

$$\frac{\partial u_z}{\partial z}+\frac{\sin\phi}{z}\frac{\partial u_\theta}{\partial\theta}+\frac{\partial u_n}{\partial n}+\frac{u_z}{z}\sin^2\phi=0, \tag{7}$$

$$u_z\frac{\partial u_z}{\partial z}+u_\theta\frac{\sin\phi}{z}\frac{\partial u_z}{\partial\theta}+u_n\frac{\partial u_z}{\partial n}-\frac{u_\theta^2}{z}\sin^2\phi=-\frac{1}{\rho}\frac{\partial p}{\partial z}-2\sin\phi\Omega u_\theta+\Omega^2 z+\nu\frac{\partial^2 u_z}{\partial n^2}, \tag{8}$$

$$u_z\frac{\partial u_\theta}{\partial z}+u_\theta\frac{\sin\phi}{z}\frac{\partial u_\theta}{\partial\theta}+u_n\frac{\partial u_\theta}{\partial n}+u_z u_\theta\frac{\sin^2\phi}{z}=-\frac{\sin\phi}{\rho z}\frac{\partial p}{\partial\theta}+2\sin\phi\Omega u_z+\nu\frac{\partial^2 u_\theta}{\partial n^2}, \tag{9}$$

where u_z, u_n, u_θ are the velocity components in the z, n, θ directions, respectively. Equation (7) is the continuity equation and (8) and (9) are the momentum equations in the z and θ directions after the boundary-layer assumptions have been applied. The simplicity of the boundary-layer equations in this geometry should be noted. This relative simplicity, in comparison with the analyses of Horlock & Wordsworth (1965) and Miyake & Fujita (1974), is a result of the choice of an appropriate co-ordinate system. Following Miyake & Fujita the velocity in the free-stream is taken to have streamlines which are the intersection of the blade surface and a circular cylinder whose axis is the axis of rotation. Thus the free-stream velocity has components

$$(W_z, W_n, W_\theta)=(0, 0, [U^2+(\Omega z)^2]^{\frac{1}{2}}). \tag{10}$$

It is then readily shown that

$$\partial p/\partial z=\partial p/\partial\theta=0. \tag{11}$$

Thus, as noted above, the static pressure is constant throughout the boundary layer (to the order of the usual boundary-layer assumptions). For the purposes of solution the θ-momentum equation may be written more conveniently as

$$u_z\frac{\partial}{\partial z}\left\{u_\theta\frac{\sin\phi}{z}\right\}+u_\theta\frac{\sin\phi}{z}\frac{\partial}{\partial\theta}\left\{u_\theta\frac{\sin\phi}{z}\right\}+u_n\frac{\partial}{\partial n}\left\{u_\theta\frac{\sin\phi}{z}\right\}+2u_z\frac{\sin^2\phi}{z}\left\{u_\theta\frac{\sin\phi}{z}-\Omega\right\}=\nu\frac{\partial^2}{\partial n^2}\left\{u_\theta\frac{\sin\phi}{z}\right\}. \tag{12}$$

Following Miyake & Fujita, a solution is sought in the form

$$u_\theta\sin\phi/\Omega z=\sum_{k=0}^{\infty}\theta^k\tilde{u}_k=\sum_{k=0}^{\infty}\theta^k u_k, \tag{13a}$$

$$u_n/\Omega z=\frac{\delta}{\epsilon L}\sum_{k=0}^{\infty}\theta^k\tilde{v}_k=\sum_{k=0}^{\infty}\theta^k v_k \tag{13b}$$

and

$$u_z/\Omega z=\sum_{k=1}^{\infty}\theta^k\tilde{w}_k=\sum_{k=1}^{\infty}\theta^k w_k, \tag{13c}$$

where

$$\theta=\epsilon\tilde{\theta},\quad n=\delta\tilde{n},\quad z=L\tilde{z}, \tag{14}$$

and quantities denoted by a tilde are of order unity. Thus ϵ is a measure of the distance from the leading edge, δ is a measure of the boundary-layer thickness ($\delta\sim[\nu\epsilon/\Omega]^{\frac{1}{2}}$) and L is a measure of the radial location. The quantity given by (13a) is the stream-

wise velocity component in the boundary layer, u_θ, divided by the free-stream streamwise velocity. Substituting series expansions of the form (13) into the boundary-layer equations gives

$$\frac{1}{z}\frac{\partial}{\partial\theta}(\theta^k u_k)+\frac{\partial}{\partial n}(\theta^k v_k) = -\frac{1}{z}\frac{\partial}{\partial z}(z\theta^{k-1}w_{k-1})-\theta^{k-1}w_{k-1}\frac{\sin^2\phi}{z}, \tag{15}$$

$$\sum_{m=0}^{k}\left\{\frac{\theta^m}{z}u_m\frac{\partial}{\partial\theta}(\theta^{k-m}w_{k-m})+\theta^m v_m\frac{\partial}{\partial n}(\theta^{k-m}w_{k-m})+\frac{\theta^{m-1}}{z}w_{m-1}\frac{\partial}{\partial z}(z\theta^{k-m}w_{k-m})\right\}$$
$$= \frac{\nu}{\Omega z}\frac{\partial^2}{\partial n^2}(\theta^k w_k)+\frac{\theta^{k-1}}{z}\left(\sum_{m=0}^{k-1}u_m u_{k-m-1}\right)-\frac{2\theta^{k-1}}{z}u_{k-1}+\frac{\delta_{1k}}{z} \tag{16}$$

and

$$\sum_{m=0}^{k}\left\{\frac{\theta^m}{z}u_m\frac{\partial}{\partial\theta}(\theta^{k-m}u_{k-m})+\theta^m v_m\frac{\partial}{\partial n}(\theta^{k-m}u_{k-m})+\theta^{m-1}w_{m-1}\frac{\partial}{\partial z}(\theta^{k-m}u_{k-m})\right\}$$
$$= \frac{\nu}{\Omega z}\frac{\partial^2}{\partial n^2}(\theta^k u_k)-\frac{2\sin^2\phi}{z}\theta^{k-1}\left\{\left(\sum_{m=0}^{k-1}u_m w_{k-m-1}\right)-w_{k-1}\right\}, \tag{17}$$

with $w_{-1} = w_0 = 0$ and δ_{ij} being the Kronecker delta function. This system of equations has been solved for several values of k. Only $k = 0, 1, 2$ are given explicitly here.

Solution for $k = 0$

Equations (15) and (17) yield

$$(1/z)\,\partial u_0/\partial\theta+\partial v_0/\partial n = 0 \tag{18}$$

and

$$\frac{u_0}{z}\frac{\partial u_0}{\partial\theta}+v_0\frac{\partial u_0}{\partial n} = \frac{\nu}{\Omega z}\frac{\partial^2 u_0}{\partial n^2}. \tag{19}$$

Introducing a stream function such that

$$u_0 = \partial\psi_0/\partial n, \quad v_0 = -(\partial\psi_0/\partial\theta)/z \tag{20}$$

and letting

$$\psi_0 = (2\nu\theta/\Omega)^{\frac{1}{2}}f_0(\eta), \quad \eta = n(\Omega/2\nu\theta)^{\frac{1}{2}} \tag{21}$$

yields

$$f_0'''+f_0 f_0'' = 0, \quad f_0(0) = f_0'(0) = 0, \quad f_0'(\infty)\to 1, \tag{22}$$

where primes denote differentiation with respect to η. This is the Blasius problem for the flat-plate boundary layer. Note that the solution is valid for all values of ϕ.

Solution for $k = 1$

Equations (15), (16) and (17) become

$$(1/z)\,\partial(\theta u_1)/\partial\theta+\partial(\theta v_1)/\partial n = 0, \tag{23}$$

$$\frac{u_0}{z}\frac{\partial}{\partial\theta}(\theta w_1)+v_0\frac{\partial}{\partial n}(\theta w_1)-\frac{(u_0-1)^2}{z}+\frac{\nu}{\Omega z}\frac{\partial^2}{\partial n^2}(\theta w_1), \tag{24}$$

$$\frac{u_0}{z}\frac{\partial}{\partial\theta}(\theta u_1)+\frac{\theta u_1}{z}\frac{\partial u_0}{\partial\theta}+v_0\frac{\partial}{\partial n}(\theta u_1)+\theta v_1\frac{\partial u_0}{\partial n} = \frac{\nu}{\Omega z}\frac{\partial^2}{\partial n^2}(\theta u_1). \tag{25}$$

As before a stream function is introduced such that

$$\theta u_1 = \partial\psi_1/\partial n, \quad \theta v_1 = -(\partial\psi_1/\partial\theta)/z. \tag{26}$$

Letting

$$\psi_1 = (2\nu\theta^3/\Omega)^{\frac{1}{2}} f_1(\eta), \tag{27}$$

yields

$$f_1''' + f_0 f_1'' - 2f_0' f_1' + 3f_0'' f_1 = 0, \quad f_1(0) = f_1'(0) = 0, \quad f_1'(\infty) \to 0. \tag{28}$$

This problem has the unique solution $f_1(\eta) = 0$, so that

$$u_1 = v_1 = 0. \tag{29}$$

It is found in general that

$$\left.\begin{aligned} u_{2k+1} = v_{2k+1} = 0, \\ w_{2k} = 0, \end{aligned}\right\} \quad k = 0, 1, 2, \ldots. \tag{30}$$

Letting

$$w_1 = g_1'(\eta) \tag{31}$$

and using (23), $g_1(\eta)$ satisfies the problem

$$g_1''' + f_0 g_1'' - 2f_0' g_1' + 2(f_0' - 1)^2 = 0, \quad g_1(0) = g_1'(0) = 0, \quad g_1'(\infty) \to 0. \tag{32}$$

Note that the solution for $g_1(\eta)$, which determines the lowest-order cross-flow velocity, is also independent of the twist angle ϕ.

Solution for $k = 2$

Equations (15) and (17) give

$$\frac{1}{z}\frac{\partial}{\partial\theta}(\theta^2 u_2) + \frac{\partial}{\partial n}(\theta^2 v_2) = -\frac{1}{z}\frac{\partial}{\partial z}(z\theta w_1) - \theta w_1 \frac{\sin^2\phi}{z}, \tag{33}$$

and

$$\frac{u_0}{z}\frac{\partial}{\partial\theta}(\theta^2 u_2) + \frac{\theta^2 u_2}{z}\frac{\partial u_0}{\partial\theta} + v_0\frac{\partial}{\partial n}(\theta^2 u_2) + \theta^2 v_2\frac{\partial u_0}{\partial n} + \theta w_1\frac{\partial u_0}{\partial z} + \frac{2\sin^2\phi}{z}\theta w_1(u_0 - 1) = \frac{\nu}{\Omega z}\frac{\partial^2}{\partial n^2}(\theta^2 u_2). \tag{34}$$

An expansion in powers of $\cos^2\phi$ is introduced such that

$$u_2 = \sum_{l=0}^{\infty} u_{2,2l} c^{2l}, \tag{35a}$$

$$v_2 = \sum_{l=0}^{\infty} v_{2,2l} c^{2l} \tag{35b}$$

in which $c^2 = \cos^2\phi$. To order $(c^2)^0$ the equations are

$$(1/z)\,\partial(\theta^2 u_{20})/\partial\theta + \partial(\theta^2 v_{20})/\partial n = -2\theta w_1/z, \tag{36}$$

$$\frac{u_0}{z}\frac{\partial}{\partial\theta}(\theta^2 u_{20}) + \frac{\theta^2}{z}u_{20}\frac{\partial u_0}{\partial\theta} + v_0\frac{\partial}{\partial n}(\theta^2 u_{20}) + \theta^2 v_{20}\frac{\partial u_0}{\partial n} + \frac{2\theta w_1}{z}(u_0 - 1) = \frac{\nu}{\Omega z}\frac{\partial^2}{\partial n^2}(\theta^2 u_{20}). \tag{37}$$

Introducing a stream function so that

$$\theta^2 u_{20} = \partial\psi_{20}/\partial n, \quad \theta^2 v_{20} = -\{\partial\psi_{20}/\partial\theta + 2(2\nu\theta^3/\Omega)^{\frac{1}{2}} g_1\}/z \tag{38}$$

with

$$\psi_{20} = (2\nu\theta^5/\Omega)^{\frac{1}{2}} f_{20}(\eta), \tag{39}$$

means $f_{20}(\eta)$ satisfies the problem

$$\left.\begin{aligned} f_{20}''' + f_0 f_{20}'' - 4f_0' f_{20}' + 5f_0'' f_{20} = 4(f_0' - 1)g_1' - 4f_0'' g_1, \\ f_{20}(0) = f_{20}'(0) = f_{20}'(\infty) = 0. \end{aligned}\right\} \tag{40}$$

This procedure may be repeated for higher orders of (c^2) and higher values of k. The definitions of the higher-order stream functions and the problems they satisfy are given in the appendix. The streamwise velocity has been found to be of the form

$$\begin{aligned} u_\theta \sin\phi/\Omega z &= u_0 + \theta^2 u_2 + \theta^4 u_4 + \dots \\ &= f_0' + \theta^2(f_{20}' + c^2 f_{22}') + \theta^4(f_{40}' + c^2 f_{42}' + c^4 f_{44}') + \dots \end{aligned} \tag{41}$$

and the spanwise or cross-flow velocity is found to be

$$\begin{aligned} u_z/\Omega z &= \theta w_1 + \theta^3 w_3 + \theta^5 w_5 + \dots \\ &= \theta g_1' + \theta^3(g_{30}' + c^2 g_{32}') + \theta^5(g_{50}' + c^2 g_{52}' + c^4 g_{54}') + \dots . \end{aligned} \tag{42}$$

Defining a streamwise skin-friction coefficient as

$$c_{f\theta} = \mu[\partial u_\theta/\partial n]_{n=0}/\tfrac{1}{2}\rho(\Omega z/\sin\phi)^2, \tag{43}$$

and since $\Omega z/\sin\phi = W_\theta$, it is readily shown that

$$c_{f\theta} Re^{\frac{1}{2}} = \sqrt{2}\{f_0''(0) + \theta^2[f_{20}''(0) + c^2 f_{22}''^{(0)}(0)] + \theta^4[f_{40}''(0) + c^2 f_{42}''(0) + c^4 f_{44}''(0)] + \dots\} \tag{44}$$

where the Reynolds number is based on the distance from the leading edge along a helix of angle ϕ. Thus the Reynolds number is given by

$$Re = W_\theta x/\nu = z^2\theta/\nu \sin^2\phi. \tag{45}$$

Similarly the spanwise skin friction coefficient may be defined as

$$c_{fz} = \mu[\partial u_z/\partial n]_{n=0}/\tfrac{1}{2}\rho(\Omega z/\sin\phi)^2 \tag{46}$$

and

$$\begin{aligned} c_{fz} Re^{\frac{1}{2}} &= \sqrt{2}\sin\phi\{\theta g_1''(0) + \theta^3[g_{30}''(0) + c^2 g_{32}''(0)] \\ &\quad + \theta^5[g_{50}''(0) + c^2 g_{52}''(0) + c^4 g_{54}''(0) + \dots\}. \end{aligned} \tag{47}$$

3. Results

The systems of ordinary differential equations for the stream function of the primary flow $f_{2k,2l}$ and the cross-flow $g_{2k+1,2l}$ have been solved numerically. The numerical scheme and computer program used were those developed by Nachtsheim & Swigert (1965). The equations were written as a system of first-order differential equations and integrated with a predictor–corrector (Adams–Moulton) subroutine using one correction per step and a fixed increment. The step-size, $\Delta\eta$, was 0·0625 and the asymptotic boundary conditions were applied at $\eta = 6{\cdot}0$. The solution was programmed in double precision and the solutions up to $k = 5$ were obtained in 2·11 seconds of processing time on an IBM 3033 system. The unknown initial conditions at the wall determining the slope of the velocity profiles are given in table 1.

The functions $f_{2k,2l}$ and $g_{2k+1,2l}$ are shown in figures 2 and 3, respectively. The function f_0' is the Blasius solution for the flat-plate boundary-layer velocity. The function g_1', which determines the cross-flow velocity to its lowest order, is identical with that obtained by Horlock & Wordsworth (1965) with $\sin\phi = 1$ and $z\Omega/U = -1$ ($P = 1, Q = -1$, in their notation). This is also the solution to Fogarty's (1951) problem of the rotating flat plate although, as noted by Horlock & Wordsworth (1965) the choice of co-ordinate system omits a term involving $(f_0')^2$. The mean velocity

$f''_0(0)$	0·46960	$g'_1(0)$	0·94073
$f''_{20}(0)$	0·78997	$g'_{30}(0)$	−0·67246
$f''_{22}(0)$	−0·67202	$g'_{32}(0)$	0·50130
$f''_{40}(0)$	−1·28978	$g'_{50}(0)$	1·32099
$f''_{42}(0)$	1·82201	$g'_{52}(0)$	−1·73799
$f''_{44}(0)$	−0·56169	$g'_{54}(0)$	0·48453

TABLE 1. Initial boundary conditions at $\eta = 0$ to five decimal places.

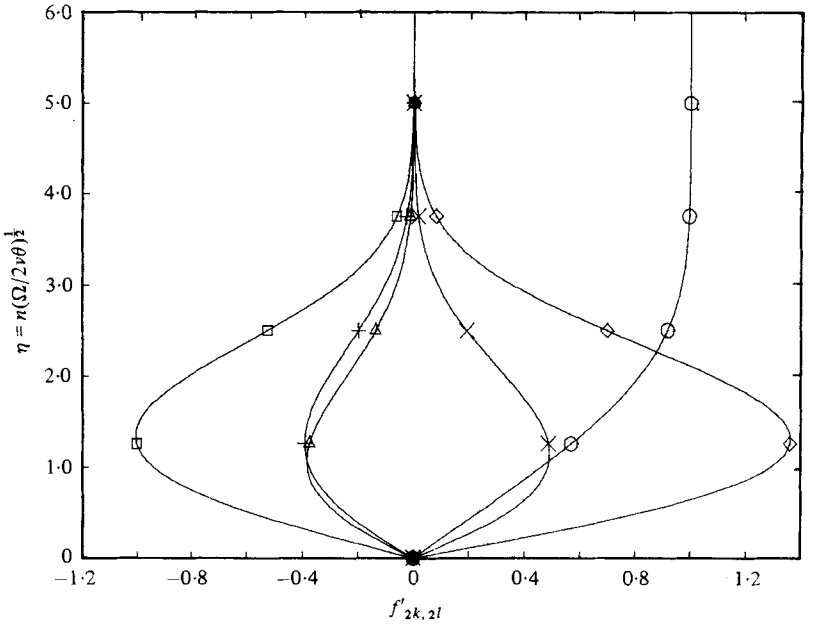

FIGURE 2. Streamwise velocity profile shapes, $f'_{2k,2l}$. f'_0, ○—○; f'_{20}, ×—×; f'_{22}, △—△; f'_{40}, □—□; f'_{42}, ◇—◇; f'_{44}, +—+.

profiles in the θ and z directions for $\phi = 90°$ and $\phi = 45°$ are shown in figures 4 and 5, respectively. $\phi = 90°$ represents the blade at large radius. As the polar distance from the leading edge increases so the streamwise velocity gradient at the wall increases and the magnitude of the cross-flow velocity increases. Since the differences with radius or twist angle are small, changes are better seen by considering the functions $f_{2k,2l}$ and $g_{2k+1,2l}$ in figures 2 and 3. If only terms of up to order θ^2 are considered for the streamwise profiles then for $\phi = 90°$ the scaled velocity, $u_\theta \sin\phi/\Omega z$, is increased at all values of η since f'_{20} is positive. However as ϕ decreases this increase is reduced since f'_{22} is always negative. Close to $\phi = 0$ there is almost complete cancellation of the order-θ^2 terms and the profile shape is nearly identical with the Blasius solution. A similar behaviour is observed for the cross-flow velocity profile up to order θ^3; however since g'_{30} is negative and g'_{32} is positive the smallest scaled cross-flow velocities, $u_z/\Omega z$, occur for $\phi = 90°$, at large radius. Thus the shape of the boundary-layer profiles are seen to be slowly varying functions of θ and z, since ϕ is only a function of z. Variations with z only occur to order θ^2 for the streamwise velocity component u_θ and to order θ^3 for the cross-flow or radial velocity component u_z. However, it

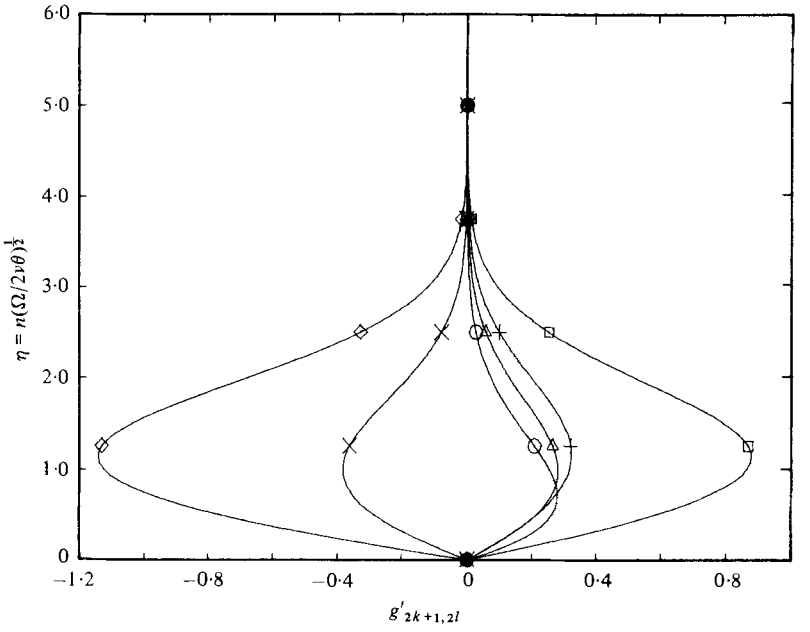

FIGURE 3. Cross-flow velocity profile shapes, $g'_{2k+1,2l}$: g'_1, ○—○; g'_{30}, ×—×; g'_{32}, △—△; g'_{50}, □—□; g'_{52}, ◇—◇; g'_{54}, +—+.

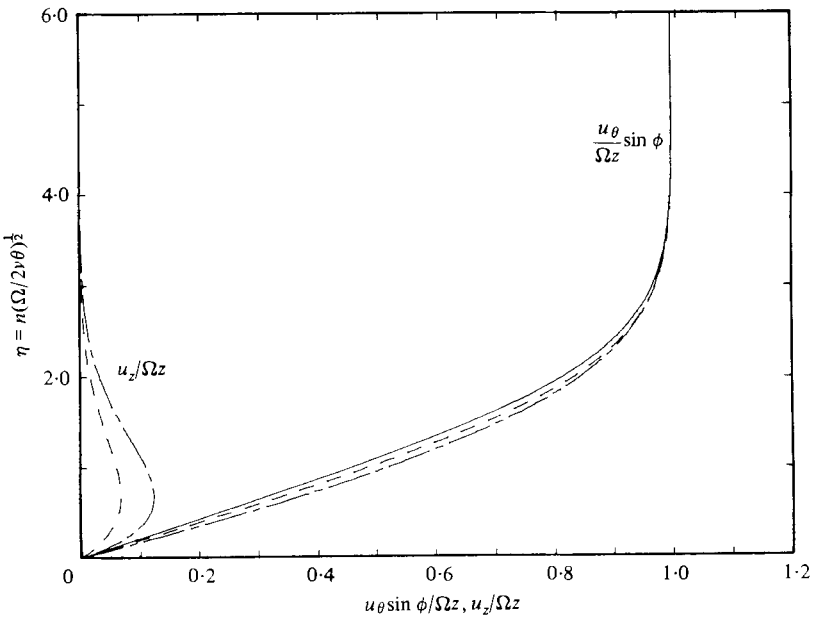

FIGURE 4. Streamwise ($u_\theta \sin\phi/\Omega z$) and radial ($u_z/\Omega z$) velocity profiles for various polar distances from the blade leading edge; $\phi = 90{\cdot}0$. —, $\theta = 0{\cdot}0$; - - - -, $\theta = \pi/12$; — — —, $\theta = \pi/6$.

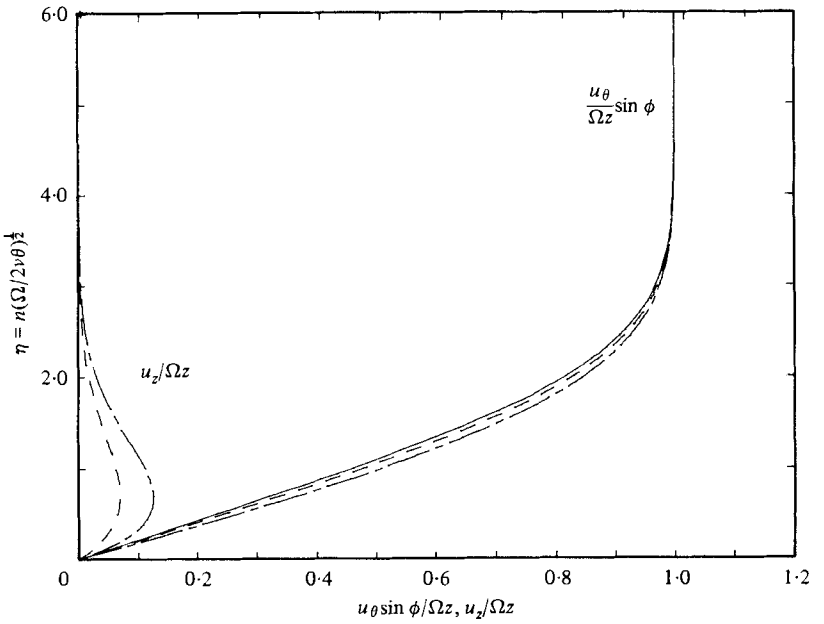

FIGURE 5. Streamwise ($u_\theta \sin\phi/\Omega z$) and radial ($u_z/\Omega z$) velocity profiles for various polar distances from the blade leading edge; $\phi = 45°$. —, $\theta = 0{\cdot}0$; – – – –, $\theta = \pi/12$; — – —, $\theta = \pi/6$.

should be emphasized that in these profiles the velocity components have been scaled by the local free-stream velocity magnitude, $\Omega z/\sin\phi$ in the case of u_θ and the azimuthal free-stream velocity component Ωz in the case of u_z. These variations in the profile shapes are also seen if the skin friction coefficient variations, given by (44) and (47), are examined. The streamwise skin friction coefficient, $c_{f\theta}$, is shown in figure 6. At the blade leading edge it is independent of the twist angle ϕ and is that for the Blasius flat-plate boundary layer, 0·6641. Its value increases with distance from the leading edge as observed in the mean velocity profiles. The greatest increases occur at large blade radius, $\phi = 90°$. The distance from the leading edge along the blade surface in the streamwise direction is related to θ and ϕ by

$$x/z = \theta/\sin\phi. \tag{48}$$

Thus for $\phi = 90°$, $x/z = \theta$. This enables comparison of the present results with those of Miyake & Fujita (1974). For the range of parameters they considered their results are the same as the present values since for $\phi = 90°$ the blade geometries are identical. For $\phi = 90°$ Miyake & Fujita computed values for $c_{f\theta}$ up to $\theta = 0{\cdot}2$. Only their calculation for $\theta = 0{\cdot}2$ and $\phi = 90°$ is shown for clarity. It should be noted that for a fixed value of θ the distance along a blade element at a given radius increases with radius. Thus at a fixed value of x from the leading edge higher values of streamwise skin friction coefficient occur at smaller radii. From equations (2) and (48) the value of θ for a fixed value of x is inversely proportional to $\cos\phi$. Thus, for example, with $\phi = 60°$ and $\theta = 0{\cdot}2$, $x = 0{\cdot}4(U/\Omega)$ and $c_{f\theta} = 0{\cdot}69$. With $x = 0{\cdot}4(U/\Omega)$ and $\phi = 45°$ then $\theta = 0{\cdot}2828$ and $c_{f\theta} = 0{\cdot}71$. The variation of the cross-flow skin friction coefficient, c_{fz}, is shown in figure 7. At the leading edge the value is zero since there is no cross-flow. The value of c_{fz} decreases with decreasing ϕ. Though as noted above for the

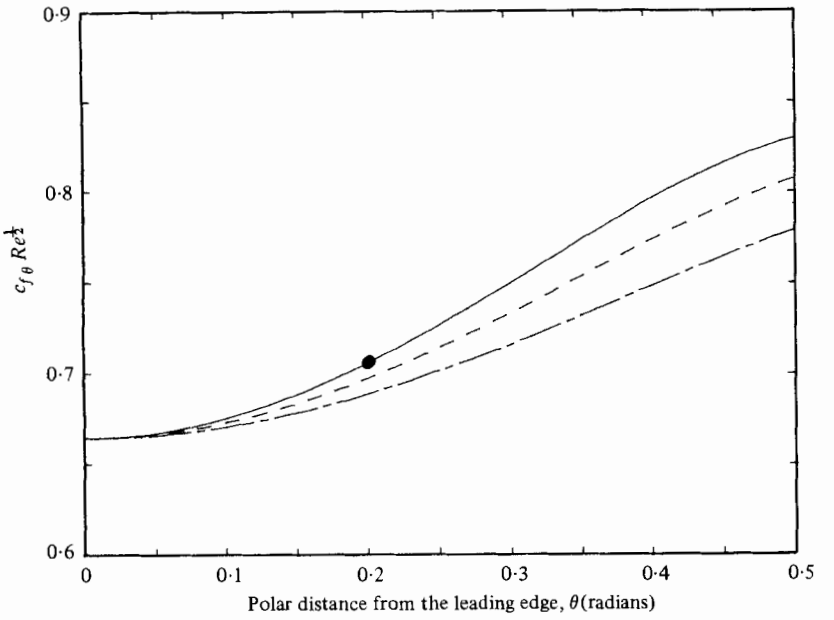

FIGURE 6. Variation of streamwise skin friction coefficient ($c_{f\theta}\,Re^{\frac{1}{2}}$) with polar distance from the blade leading edge. —, $\phi = 90°$; – – –, $\phi = 60°$; — — —, $\phi = 45°$. ●, Miyake & Fujita (1974), $\phi = 90°$, $\theta = 0{\cdot}2$.

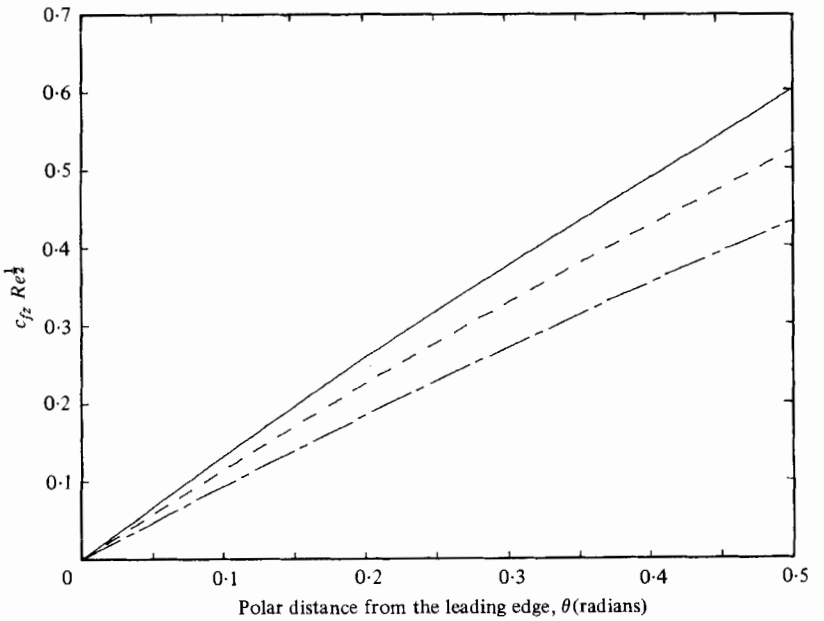

FIGURE 7. Variation of radial or cross-flow skin friction coefficient ($c_{fz}\,Re^{\frac{1}{2}}$) with polar distance from the blade leading edge. —, $\phi = 90°$; – – – –, $\phi = 60°$; — — —, $\phi = 45°$.

streamwise coefficient, the value increases with decreasing ϕ for fixed helical distances x from the leading edge. The magnitude of c_{fz} approaches the magnitude of the streamwise coefficient, $c_{f\theta}$, for values of θ about 0·5.

4. Conclusions

The analysis has shown that by appropriate choice of the co-ordinate system the three-dimensional boundary layer on a rotating blade may be calculated without restricting the results to blades with no twist as in Horlock & Wordsworth (1965), or to twisted blades with no streamwise curvature as in Miyake & Fujita (1974), which results in a non-zero pressure gradient. The twisted helical blade analysed in this paper was shown to be a screw surface and the resulting boundary layer is the analogue, in a rotating reference frame, of the zero-pressure-gradient flat plate boundary layer. It should be emphasized that though the numerical results of the present paper are similar to those obtained by Miyake & Fujita (1974) the choice of co-ordinate system enables the effects of blade stagger and twist for a workless, or zero-pressure-gradient blade boundary layer to be readily developed. The boundary-layer calculations in this paper serve several purposes. They provide the initial conditions for the calculation of the wake behind a rotor blade of finite chord, with the geometry of the present paper. They provide the basis for comparison as verification for other computational methods which are more readily extended to variations of the present simple geometry. If transition from laminar to turbulent flow in the boundary layer is taken to be the result of small disturbances of the Tollmein–Schlichting type, rather than due to disturbances in the free stream, then the present analysis provides a simple primary flow which, in the limit of zero rotation, is the Blasius flat-plate boundary layer.

The author is grateful to Dr A. Solan and Dr M. Ungarish, Technion-Israel Institute of Technology, for noting an algebraic error in the original manuscript. The support of NASA Lewis Research Centre under grant number NSG 3265 is also acknowledged.

Appendix

The definitions of the higher-order stream functions and the problems they satisfy are summarized below:

$$\theta^2 u_{22} = \partial\psi_{22}/\partial n, \quad \theta^2 v_{22} = -\{\partial\psi_{22}/\partial\theta - (2\nu\theta^3/\Omega)^{\frac{1}{2}} g_1\}/z, \tag{A 1}$$

with

$$\psi_{22} = (2\nu\theta^5/\Omega)^{\frac{1}{2}} f_{22} \tag{A 2}$$

and

$$f'''_{22} + f_0 f''_{22} - 4f'_0 f'_{22} + 5f''_0 f_{22} = -4(f'_0 - 1)g'_1 - 4f'_0 g'_1, \tag{A 3}$$

$$f_{22}(0) = f'_{22}(0) = f'_{22}(\infty) = 0; \tag{A 4}$$

$$w_3 = g'_{30} + c^2 g'_{32} \tag{A 5}$$

where

$$g'''_{30} + f_0 g''_{30} - 6f'_0 g'_{30} = 2(g'_1)^2 - 4g_1 g''_1 - 5f_{20} g''_1 + 2f'_{20} g'_1 - 4(f'_0 - 1)f'_{20}, \tag{A 6}$$

$$g'''_{32} + f_0 g''_{32} - 6f'_0 g'_{32} = 2g_1 g''_1 - 5f_{22} g''_1 + 2f'_{22} g'_1 - 4(f'_0 - 1)f'_{22}, \tag{A 7}$$

with

$$g_{30}(0) = g'_{30}(0) = g_{32}(0) = g'_{32}(0) = g'_{30}(\infty) = g'_{32}(\infty) = 0; \tag{A 8}$$

$$u_4 = u_{40} + c^2 u_{42} + c^4 u_{44} \tag{A 9a}$$

and

$$v_4 = v_{40} + c^2 v_{42} + c^4 v_{44}, \tag{A 9b}$$

$$\theta^4 u_{40} = \partial\psi_{40}/\partial n, \quad \theta^4 v_{40} = -\{\partial\psi_{40}/\partial n + 2(2\nu\theta^7/\Omega)^{\frac{1}{2}} g_{30}\}/z, \tag{A 10}$$

with

$$\psi_{40} = (2\nu\theta^9/\Omega)^{\frac{1}{2}} f_{40}(\eta), \tag{A 11}$$

$$f_{40}''' + f_0 f_{40}'' - 8f_0' f_{40}' + 9f_0'' f_{40} = 4(f_0' - 1) g_{30}' - 4f_0'' g_{30} - 4g_1 f_{20}'' + 4g_1' f_{20}' - 5f_{20} f_{20}'' + 4(f_{20}')^2, \tag{A 12}$$

and

$$f_{40}(0) = f_{40}'(0) = f_{40}'(\infty) = 0; \tag{A 13}$$

$$\theta^4 u_{42} = \partial\psi_{42}/\partial n, \quad \theta^4 v_{42} = -\{\partial\psi_{42}/\partial\theta - (2\nu\theta^7/\Omega)^{\frac{1}{2}} g_{30}\}/z, \tag{A 14}$$

with

$$\psi_{42} = (2\nu\theta^9/\Omega)^{\frac{1}{2}} f_{42}(\eta), \tag{A 15}$$

$$f_{42}''' + f_0 f_{42}'' - 8f_0' f_{42}' + 9f_0'' f_{42} = 4(f_0' - 1)(g_{32}' - g_{30}') + 2f_0'' g_{30} + 2g_1(f_{20}'' - 2f_{22}'') - 4g_1' f_{20}' + 8f_{20}' f_{22}' - 5f_{20} f_{22}'' - 5f_{22} f_{20}'' \tag{A 16}$$

and

$$f_{42}(0) = f_{42}'(0) = f_{42}'(\infty) = 0; \tag{A 17}$$

$$\theta^4 u_{44} = \partial\psi_{44}/\partial n, \quad \theta^4 v_{44} = -\{\partial\psi_{44}/\partial\theta + (2\nu\theta^7/\Omega)^{\frac{1}{2}} g_{32}\}/z, \tag{A 18}$$

with

$$\psi_{44} = (2\nu\theta^9/\Omega)^{\frac{1}{2}} f_{44}(\eta), \tag{A 19}$$

$$f_{44}''' + f_0 f_{44}'' - 8f_0' f_{44}' + 9f_0'' f_{44} = -4(f_0' - 1) g_{32}' - 2f_0'' g_{32} + 2g_1 f_{22}'' - 5f_{22} f_{22}'' + 4(f_{22}')^2, \tag{A 20}$$

and

$$f_{44}(0) = f_{44}'(0) = f_{44}'(\infty) = 0; \tag{A 21}$$

$$w_5 = g_{50}'(\eta) + c^2 g_{52}'(\eta) + c^4 g_{54}'(\eta), \tag{A 22}$$

where

$$g_{50}''' + f_0 g_{50}'' - 10f_0' g_{50}' = -4(f_0' - 1) f_{40}' - 4g_1 g_{30}'' + 4g_1' g_{30}' + 2g_1' f_{40}' - 4g_1'' g_{30} - 9g_1'' f_{40} - 5f_{20} g_{30}'' - 2(f_{20}')^2 + 6f_{20}' g_{30}', \tag{A 23}$$

$$g_{52}''' + f_0 g_{52}'' - 10f_0' g_{52}' = -4(f_0' - 1) f_{42}' + 2g_1 g_{30}'' - 4g_1 g_{32}'' + 2g_1' f_{42}' + 2g_1'' g_{30} - 9g_1'' f_{42} - 5f_{20} g_{32}'' + 6f_{20}' g_{32}' - 4f_{20}' f_{22}' - 5f_{22} g_{30}'' + 6f_{22}' g_{30}', \tag{A 24}$$

$$g_{54}''' + f_0 g_{54}'' - 10f_0' g_{54}' = -4(f_0' - 1) f_{44}' + 2g_1 g_{32}'' + 4g_1' g_{32}' + 2g_1' f_{44}' - 2g_1'' g_{32} - 9g_1'' f_{44} - 5f_{22} g_{32}'' - 2(f_{22}')^2 + 6f_{22}' g_{32}', \tag{A 25}$$

$$g_{50}(0) = g_{50}'(0) = g_{52}(0) = g_{52}'(0) = g_{54}(0) = g_{54}'(0) = 0, \tag{A 26}$$

and

$$g_{50}'(\infty) = g_{52}'(\infty) = g_{54}'(\infty) = 0. \tag{A 27}$$

REFERENCES

FOGARTY, L. E. 1951 The laminary boundary layer on a rotating blade. *J. Aero. Sci.* **18**, 247–252.

HORLOCK, J. H. & WORDSWORTH, J. 1965 The three-dimensional laminar boundary layer on a rotating helical blade. *J. Fluid Mech.* **23**, 305–314.

LAKSHMINARAYANA, B., JABBARI, A. & YAMAOKA, H. 1972 Turbulent boundary layer on a rotating helical blade. *J. Fluid Mech.* **51**, 545–569.

MICHAL, A. D. 1947 *Matrix and Tensor Calculus.* Wiley.

MIYAKE, Y. & FUJITA, S. 1974 A laminar boundary layer on a rotating three-dimensional blade. *J. Fluid Mech.* **65**, 481–498.

NACHTSHEIM, P. R. & SWIGERT, P. 1965 Satisfaction of asymptotic boundary conditions in numerical solutions of systems of non-linear equations of boundary layer type. *N.A.S.A. Tech. Note* D-3004.

TAN, H. S. 1953 On laminar boundary layer over a rotating blade. *J. Aero. Sci.* **20**, 780–781.

YAMAMOTO, K. & TOYOKURA, T. 1974 Analysis of the boundary layer on a workless rotating thin blade. *Bull. Japan Soc. Mech. Engrs* **17**, 1023–1029.